

# Resolving Collisions for the Gipps Car-Following Model

Leonhard Lücken<sup>1</sup>

March 1, 2022

<sup>1</sup>German Aerospace Center (DLR), Institute of Transportation Systems, Rutherfordstraße 2, 12489 Berlin, Germany

## Abstract

The Gipps car-following model is a widely used tool for studying and simulation traffic dynamics. Despite its popularity an often disregarded property is that under heterogeneous parametrization on the individual vehicles in the traffic flow, the model may produce collisions. This stands in crude contrast to the principle, from which the model was derived: drive as fast as possible while guaranteeing a safe headway in case that the leading vehicle starts braking hard. Indeed, Gipps proof for the model being collision-free only holds for ensembles of identical vehicles.

In this work we examine the circumstances leading to collisions in heterogeneous ensembles and propose a natural model extension, which conveys the original models principles to situations, where collisions occur. For these cases we present analytical and numerical results on the stability of the equilibrium flow.

## 1 Introduction

Numerical simulation is an important tool for the understanding of dynamical phenomena arising in traffic systems as, for instance, traffic jam formation and propagation. Traffic simulations can also help to predict the performance of specific road network elements or their configurations, e.g., a novel traffic light algorithm. They are valuable tools for the guidance of infrastructural planning processes as well as for the scientific evaluation of new ideas.

Microscopic traffic simulations employ simulation models, which account for each single vehicle as a separate entity with a defined position and speed at each moment [12]. In each simulation step, the vehicle's individual state is updated using a rule, which determines the vehicle's acceleration depending on its current environment. For many car-following models, it is assumed that the chosen acceleration is a function of the current positions and speeds of the vehicle itself and of its immediate leader vehicle, i.e., the vehicle driving ahead.

In this paper we study a popular car-following model, named after its inventor P.G. Gipps [6], who proposed the model in 1981. The model is based on the intuitive principle that drivers drive at the highest speed that ensures not crashing into the rear of the leader vehicle if it brakes suddenly. This clear approach for the model derivation gives a comprehensible meaning to each parameter and is one reason for the model's popularity until today.

The original model, or one of its variants, is employed in several important microscopic traffic simulators [2, 1, 7].

Although the Gipps model uses an acceleration function, which is derived from a safety principle [see Eqn. (5) below], it is well-known that for certain choices of parameters the model exhibits collisions. These collisions cannot be tied to common causes for collisions in reality but are rather a defect of the model itself. This poses problems for its application in microsimulators and different strategies were proposed for the solution [4, 8, 9]. All strategies known to the authors constrain the allowed model parameters, thereby excluding values that seem reasonable to assume under adequate circumstances given their proposed meaning.

More precisely, if the follower vehicle is disposed to brake significantly harder than the leader, the model may produce unsafe behavior even if the follower's estimate of the maximal deceleration of the leader vehicle

is correct. Wilson argued that such a parametrization is unphysical [13]. Although this may be formally correct for the original, we argue that a maximal safe following speed should exist in that situation. We propose that, instead of restricting the model parameters, one should modify the safety principle used as the starting point of its derivation. In its original form, the safety principle only requires the hypothetical gap between the leader and follower to be larger than zero when both have come to a stop. This hypothetical gap is derived by assuming braking maneuvers of leader and follower vehicles during which their hypothetical trajectories are decoupled. However, if the follower may brake harder than the leader an intersection of the hypothetical trajectories may occur, which is disregarded by Gipps' original safety principle and is the reason for the observed collisions.

In this paper we show that a natural extension of the original Gipps model exists, which is obtained when Gipps' safety principle is applied to all time points of the hypothetical braking maneuvers, and which prevents the described type of collisions. To this end, we briefly review the original model in Sec. 2 and review its derivation paying a special attention to the problematic case leading to collisions in Sec. 3. In Section 4 we present the detailed derivation of an extended model accounting for that case appropriately. Section 5 studies the equilibrium flow yielding an natural extension of the speed-headway function of the original model. The stability of the equilibrium flow in a many vehicle system is studied analytically in Sec. 6 for identical vehicles and for a heterogeneous ensemble in Section 7. In the concluding Section 8 we provide additional interpretation for our results and discuss open points.

## 2 Gipps' Original Car-Following Model

The original Gipps model [6] maps the velocity  $v(t)$  of a driver-vehicle unit to its speed  $v(t + \tau)$  attained at time  $t + \tau$  as

$$v(t + \tau) = v(t) + \tau \cdot a(t). \quad (1)$$

The positional increment is then calculated by a trapezoid rule

$$x(t + \tau) = x(t) + \tau \frac{v(t) + v(t + \tau)}{2}, \quad (2)$$

corresponding to a constant value for acceleration  $a(s) \equiv a(t) = (v(t + \tau) - v(t))/\tau$  during the interval  $s \in [t, t + \tau]$ . For the acceleration Gipps assumes the form

$$a(t) = \min(a_{\max}, a_{\text{safe}}) \quad (3)$$

Here  $a_{\max} = a_{\max}(v(t))$  is a velocity-dependent maximal acceleration and  $a_{\text{safe}}$  is a safe acceleration calculated in dependence of the current speeds and positions of the vehicle and its immediate leader vehicle, as well as several parameters described in more detail below. The maximal acceleration as defined by Gipps is

$$a_{\max}(v) = 2.5\alpha \left(1 - \frac{v}{v_{\max}}\right) \sqrt{0.025 + \frac{v}{v_{\max}}}, \quad (4)$$

with a parameter  $\alpha > 0$  describing the maximal desired acceleration of the driver. The safe acceleration  $a_{\text{safe}}$  is determined from a safety equation, which attempts to assure that the vehicle can break in time if the leading vehicle starts breaking at time  $t$  with an assumed deceleration  $\hat{B} > 0$ . Gipps formulates the safety equation assuming that the ego vehicle accelerates until  $t + \tau$  with  $a_{\text{safe}}$ , then travels with velocity  $v(t + \tau)$  until  $t + \tau + \theta$  and starts breaking with a maximal desired deceleration  $B > 0$  afterwards. Here  $\theta$  is an additional safety margin often disregarded or set to a constant proportion with respect to  $\tau$ . Gipps himself performed most of his studies only for the case  $\theta = \tau/2$ . In this work we keep  $\theta$  as a free parameter. Although it does not have an independent effect on the desired gap  $g_0$  [see Eq. (11)], which depends only on the sum  $\tau + \theta$  [see Eqn. (11) below], the value of  $\theta$  *does* change the dynamic properties of the model. For instance it has an independent influence on the stability of the equilibrium flow solution [13]. Moreover, it affects the approaching and stopping behavior of a follower vehicle. For instance, a larger value of  $\theta$  induced a smooth, or "creeping", stopping, while for  $\theta = 0$ , the stopping is performed to the point [11].

The resulting safety equation proposed by Gipps is:

$$\underbrace{\frac{v_f(t) + v_f(t + \tau)}{2} \cdot \tau}_{\text{follower's distance covered in } [t, t + \tau]} + \underbrace{v_f(t + \tau)\theta}_{\text{follower's distance covered in } [t + \tau, t + \tau + \theta]} + \underbrace{\frac{v_f(t + \tau)^2}{2B}}_{\text{follower's brake-dist}} \leq \underbrace{g(t)}_{\text{current gap}} + \underbrace{\frac{v_\ell(t)^2}{2\hat{B}}}_{\text{leader's brake-dist}}, \quad (5)$$

where  $v_f$  and  $v_\ell$  are the velocities of the following and leading vehicles and

$$g(t) = x_\ell^{\text{back}} - x_f^{\text{front}} - g_{\text{stop}} \quad (6)$$

is their front-to-back gap diminished by a minimal gap  $g_{\text{stop}} > 0$ , which should be maintained at standstill. Here  $\hat{B}$  denotes the maximal expected deceleration of the leader as estimated by the follower.

Gipps proposed the following expression<sup>1</sup> for the maximal safe following speed  $v_{\text{safe}}$  at time  $t + \tau$  obtained from equating both sides of (5) and solving for  $v(t - \tau) \geq 0$ :

$$v_{\text{safe}} = -B\left(\frac{\tau}{2} + \theta\right) + \sqrt{\left(B\left(\frac{\tau}{2} + \theta\right)\right)^2 + B\left(2g(t) - v_f(t)\tau + \frac{v_\ell(t)^2}{\hat{B}}\right)}. \quad (7)$$

The obtained value  $v_{\text{safe}}$  is then used for the dynamical update (1)-(2). Assuming  $v_{\text{safe}} \geq 0$  requires that

$$\underbrace{v_f(t)\frac{\tau}{2}}_{\substack{\text{min.dist.} \\ \text{covered till } t + \tau}} \leq \underbrace{g(t)}_{\text{current gap}} + \underbrace{\frac{v_\ell(t)^2}{2\hat{B}}}_{\text{leader's brake-dist}}. \quad (8)$$

An aspect, which is often disregarded but which is quite important for a well-behaved implementation of the model is the treatment of the case that (8) is not fulfilled [11]. It corresponds to the situation where the follower needs to stop already within the interval  $(t, t + \tau)$  thus braking with  $B_{\text{stop}}$  such that

$$\underbrace{\frac{v_f(t)^2}{2B_{\text{stop}}}}_{\substack{\text{follower's} \\ \text{brake-dist}}} = \underbrace{g(t)}_{\text{current gap}} + \underbrace{\frac{v_\ell(t)^2}{2\hat{B}}}_{\substack{\text{leader's} \\ \text{brake-dist}}},$$

i.e.,  $B_{\text{stop}} = \frac{b_\ell v_f(t)^2}{2g(t)\hat{B} + v_\ell(t)^2}$ . This leads to a special case for the update (1)-(2), where

$$v_f(t + \tau) = 0, \quad (9)$$

$$x_f(t + \tau) = x_f(t) + g(t) + \frac{v_\ell(t)^2}{2\hat{B}}. \quad (10)$$

If stopping within an update step is not implemented (it is not contained in the original model formulation) the effective deceleration rate is bounded by  $\tilde{B} = \frac{v_f(t)}{\tau}$  since the vehicle may only decelerate as much as to come to a stop exactly at time  $t + \tau$ .

### 3 Gipps' Safety Calculus Reviewed

The Gipps model is derived from considerations for the safe following gap, while seeking to prevent that the follower has to break harder than using the maximal desired deceleration rate  $B$ . Gipps already realized that for a bounded deceleration rate the model does not guarantee the maintenance of a “safe speed and distance” if no further assumptions are made. Moreover, he gave some conditions when this can be assured

<sup>1</sup>Note that Gipps did set  $\theta = \tau/2$  in at some point of the calculations in his original work.

nevertheless. First, it is clear that if the expected maximal deceleration  $\hat{B}$  of the leader is underestimated and the whole calculus is based on a faulty premise, the model cannot be expected to meet the desired property. Hence it is required that  $\hat{B} \geq B_\ell$ , where  $B_\ell$  corresponds to the actual maximal braking rate applied by the leader vehicle. Further, Gipps assumed the additional headway time  $\theta$  to equal  $\tau/2$ , which prevents collisions due to an inert approach to the desired headway time  $\tau + \theta$ .

Interestingly, Gipps' definition of "safe speed and distance" does not assure the absence of collisions. As it seems, he considers every speed and distance safe which fulfills Eq. (5) and his proof only assures that this inequality is invariant under the dynamics (1)-(2). In fact, for the case that the maximal deceleration  $B > 0$  of the follower is *larger* than the expected deceleration of a leader  $\hat{B} > 0$ , the formula (5) does not yield a guidance for the calculation of a safe distance. Indeed, even for a constant traveling speed  $v_\ell \equiv v_f \equiv v_0$ , the corresponding desired gap

$$g_0 = v_0 (\tau + \theta) + \frac{v_0^2}{2} (B^{-1} - \hat{B}^{-1}), \quad (11)$$

obtained by equating both sides of (5) may become *negative*. We have  $g_0 < 0$  iff

$$B^{-1} - \hat{B}^{-1} < -2 \frac{\tau + \theta}{v_0}. \quad (12)$$

Anyhow, it seems desirable to account for the case  $B > \hat{B}$ , e.g., to depict traffic situations where drivers choose smaller following gaps based on their willingness to apply strong braking. In the following we present strategies to deal with this deficiency of the Gipps model.

Figure 1 (a) illustrates a collision for the Gipps model due to  $B > \hat{B}$ . The leader vehicle first drives at a constant speed  $v_0 = 10\text{m/s}$  and starts braking with  $\hat{B} = 1.5\text{m/s}$  until it comes to a halt. The follower vehicle (blue trajectory along its front bumper) is controlled by a Gipps model with a maximal deceleration bounded to  $B = 4.5$ . It collides with the rear end of the leader (red trajectory along its back bumper) at  $t \approx 6\text{s}$ . After the collision a constant deceleration rate  $B$  is applied. Note that the vehicle comes to a halt at a position well before the leader's stop position as required by (5).

In Fig. 1 (b) the lack of safety is resolved by artificially increasing the deceleration rate taken into account for the leader in (7) to

$$\hat{B}_{\max} = \max\{B, \hat{B}\}. \quad (13)$$

This effectively ignores the peculiarities of the situation  $B > \hat{B}$  [see Section 7]. In (c) the collision is avoided by using an exact formula for the safe following distance in the case  $B > \hat{B}$ , which is presented below. This extended model is capable to produce smaller, though safe, headways for the situation  $B > \hat{B}$ .

## 4 An Extension of the Gipps Model for $B > \hat{B}$

In this section we give here an exact formula for the safe speed for the situation  $B > \hat{B}$ , i.e.  $\Delta B = \hat{B} - B < 0$ . In this approach we follow Gipps' original safety concept, which was based on Eqn. (5), as close as possible and extend it by the requirement that  $g(t) > 0$  can be achieved without braking harder than  $B$ . As argued above [see Eqs. (11)-(12)] the latter is not assured by satisfying (5) if  $B > \hat{B}$ .

To derive the corresponding value of  $v_f(t+\tau) = v_{\text{safe}}$  we follow the reasoning sketched in Sec. 2, considering a follower and a leader vehicle described by their positions and speeds  $(x_f, v_f)$  and  $(x_\ell, v_\ell)$ . Without loss of generality we consider the situation to be initialized at  $t_0 = 0$ . The initial state is denoted by

$$(x_{f,0}, v_{f,0}) := (x_f(0), v_f(0)), \quad (x_{\ell,0}, v_{\ell,0}) := (x_\ell(0), v_\ell(0)).$$

As for the original model, the target speed is selected based on the hypothesized scenario that the leader starts braking with rate  $\hat{B}$  at  $t = 0$ . To denote the expected states in this scenario we use notations  $v_{f,1} = v_f(t_1)$ ,  $x_{\ell,2} = x_\ell(t_2)$ , etc., with time points

$$t_1 = \tau, \text{ and } t_2 = \tau + \theta.$$

As a shorthand, we introduce the following notation for the corresponding intervals  $I_j$  of potentially different values for the follower's acceleration rate  $a_f$ :

- $I_0 = (0, t_1)$ , where  $a_f(t) \equiv \alpha$  with  $\alpha$  to be determined,

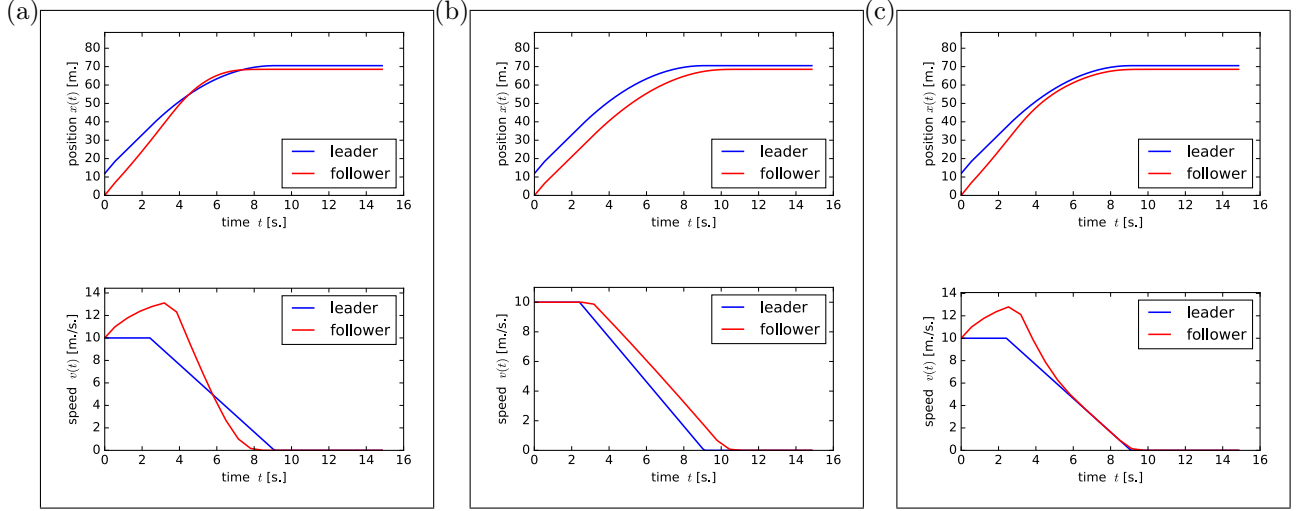


Figure 1: Comparison of trajectories for different implementations for the case that the follower has a higher maximal deceleration rate than the leader, i.e.,  $B > \hat{B} = B_\ell$ . The parameters for all cases are  $\tau = 0.66\text{s}$ ,  $\theta = 0.33\text{s}$ ,  $\hat{B} = B_\ell = 1.5\text{m/s}^2$ ,  $B = 4.5\text{m/s}^2$ , and  $g_{\text{stop}} = 2\text{m}$ ; The vehicles are inserted at an initial speed of  $v_0 = 10\text{m/s}$  and with an initial temporal headway of  $h = \vartheta + g_{\text{stop}}/v_0 = 1.2\text{s}$ , which would be stationary for  $\hat{B} = B$ . The leader vehicle travels at a speed of  $10\text{m/s}$ . At  $x \approx 50\text{m}$  it starts breaking at rate  $B_\ell$  until its back bumper comes to halt at  $x_{\text{stop}} = 80\text{m}$  (red trajectory). The follower vehicle (blue trajectory) is controlled by a Gipps model [with different strategies for  $B > \hat{B}$  and bounded deceleration rates, see main text] and its front comes to a halt at  $x = 78\text{m} = x_{\text{stop}} - g_{\text{stop}}$ .

- $I_1 = (t_1, t_2)$ , where  $a_f(t) \equiv 0$ ,
- $I_2 = (t_2, \infty)$ , where  $a_f(t) \equiv -B$ .

The computations in this section are more involved than for the case  $B \leq \hat{B}$  because more cases have to be distinguished. There are two types of important events in a collision free situation. Firstly, the expected stopping times  $t_{s,f}$  and  $t_{s,\ell}$  of the vehicles. Here, the leader's stopping time (when constant braking with rate  $\hat{B}$  is assumed) is

$$t_{s,\ell} = \frac{v_{\ell,0}}{\hat{B}}. \quad (14)$$

In addition to the stopping times the case  $B > \hat{B}$  allows for another type of event, namely a tangency of the vehicles' trajectories while both are moving at positive speed, i.e., at some moment  $t = t_{\parallel} < \min\{t_{s,f}, t_{s,\ell}\}$ . The occurrence of such a tangency can be determined from the condition

$$g(t_{\parallel}) = g'(t_{\parallel}) = 0. \quad (15)$$

Note that the reason for the absence of tangencies in the case  $B \leq \hat{B}$  is that the evolution of the gap  $g(t)$  is convex, i.e.  $g''(t) \leq 0$ , for  $t < t_{s,\ell}$  [see Fig. 2]. For  $B > \hat{B}$ , tangencies may occur within  $I_0$  and  $I_2$ , and this implies that more than one type of upper bound on the value of the acceleration  $\alpha$  within  $I_0$  has to be considered. Figure 2 shows the three different cases that may occur (excluding cases, where a stop within  $I_0$  is necessitated).

A necessary condition for the existence of a tangency at time  $t_{\parallel,j}$  in an interval  $I_j$ ,  $j = 0, 2$ , is that the gap is concave in  $I_j$  and decreases at interval begin. Therefore no tangency occurs in  $I_1$ , where the gap is always convex. A potential tangency at time  $t_{\parallel,j} < t_{s,\ell}$  defines an upper bound  $\alpha_j$  for  $\alpha$ . Formally, we can even obtain  $t_{\parallel,j} > t_{s,\ell}$  if the vehicles' deceleration is extrapolated beyond their stopping times, such that the tangency would occur for negative values of the speed. In that case, the reasoning according to (5) has to be applied to obtain the appropriate bound  $\alpha_j$  on  $\alpha$ , i.e.,  $\alpha_j = (v_{\text{safe}} - v_{f,0})/\tau$  with  $v_{\text{safe}}$  from (7), or  $\alpha_j = B_{\text{stop}}$  corresponding to the stopping update (9)–(10). In the following we will derive the constraints for

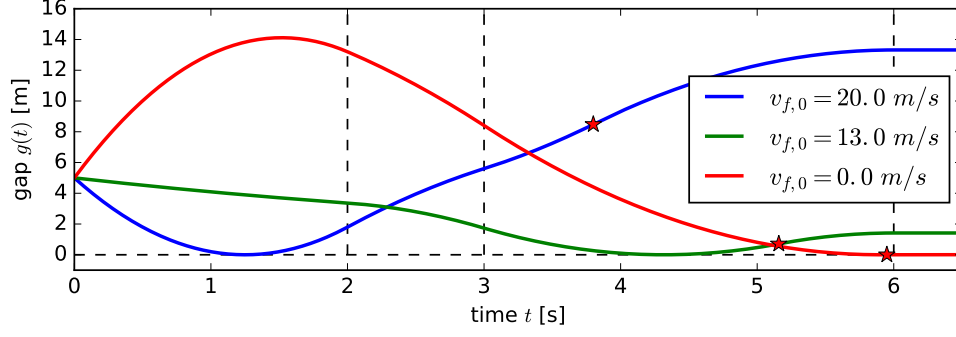


Figure 2: Three different hypothetical evolutions for the gap  $g(t)$  illustrating the different possible limiting cases for the follower's acceleration  $\alpha$  for  $t \in I_0 = (0, \tau)$ . The different cases are triggered by varying the initial speed  $v_{f,0}$  of the follower, while keeping constant the initial speed  $v_{\ell,0} = 12\text{m/s}$  of the leader and the initial gap  $g_0 = 5\text{m}$ . The blue trajectory corresponds to the case where the follower initially travels with a much larger speed  $v_{f,0} = 20\text{m/s}$  than the leader. Here, the limiting factor for the acceleration  $\alpha$  during  $I_0$  is the possible tangency within  $I_0$ . For a lower initial speed  $v_{f,0} = 13\text{m/s}$  the situation changes since for this case a tangency at time  $t = t_{\parallel,2} > t_2$  is prohibiting a higher acceleration. The red trajectory shows the hypothetical evolution of  $g(t)$  when the follower is stopped initially, i.e.,  $v_{f,0} = 0$ . In this case no tangency can occur until the leader would have stopped at  $t_{s,\ell} = 6\text{s}$ , when constantly braking with rate  $\hat{B} = 2\text{m/s}^2$ . The other model parameters were set to  $B = 4\text{m/s}^2$ ,  $\tau = 2\text{s}$ , and  $\theta = 1\text{s}$ . Red star-shaped markers indicate the extrapolated stopping times  $t_{f,s}$  of the follower for the different trajectories.

the intervals  $I_0$  and  $I_2$ , i.e.,  $\alpha_0$  and  $\alpha_2$ .

**Interval  $I_0$ .** The expected evolution of the gap  $g(t)$  for  $t \leq \tau$  is

$$g(t) = g_0 + g'_0 t - \left( \alpha + \hat{B} \right) \frac{t^2}{2}, \quad (16)$$

with  $g'_0 = g'(0) = v_{\ell,0} - v_{f,0}$  and  $g_0 = g(0) \geq 0$ . A tangency for the vehicle's trajectories within  $I_0$  requires that there exists  $t_{\parallel,0} \in I_0$  such that  $g(t_{\parallel,0}) = 0$  and

$$0 = g'(t_{\parallel,0}) = g'_0 - \left( \alpha + \hat{B} \right) t_{\parallel,0}.$$

Hence,  $t_{\parallel,0} = \frac{g'_0}{\alpha + \hat{B}}$ . Inserting this into (16) and solving  $g(t_{\parallel,0}) = 0$  for  $\alpha$  yields

$$\alpha_0 = -\frac{g_0'^2}{2g_0} - \hat{B}. \quad (17)$$

Thus,

$$t_{\parallel,0} = -\frac{2g_0}{g'_0}. \quad (18)$$

If  $0 \leq t_{\parallel,0} \leq \min\{t_{s,\ell}, \tau\}$ , it is required that  $\alpha \leq \alpha_0$ . If instead  $t_{s,\ell} \leq \tau$  and  $t_{\parallel,0} \notin (0, t_{s,\ell})$ , we compute the follower's next step as for the original model. Note that  $t_{\parallel,0} > 0$  requires  $g'_0 < 0$ . Further,  $v_{f,0} + \alpha\tau$  indicates that a stop is required within  $I_0$  for the follower. In this case the following update is to be applied:

$$v(t + \tau) = 0, \quad (19)$$

$$x(t + \tau) = x_{0,f} + \frac{v_{f,0}^2}{2\alpha_0}. \quad (20)$$

**Interval  $I_1$ .** First, we observe that if the leader has come to a halt at the end of  $I_1$ , i.e.,  $t_{s,\ell} < t_2$ , further tangencies can be disregarded as they could only occur in  $I_2$  and the classical Gipps reasoning may be applied

to obtain a bound  $\alpha_2 = (v_{\text{safe}} - v_{f,0})/\tau$  with  $v_{\text{safe}}$  according to (7). Note that the constraint  $\alpha \leq \alpha_0$ , which is applied if  $0 \leq t_{\parallel,0} \leq \min\{t_{s,\ell}, \tau\}$ , may still induce a different behavior than for the original model if  $\alpha_0 < \alpha_2$ .

If no stop must be performed by the follower within  $I_0$  and  $t_{s,\ell} > t_2$ , the evolution of the gap  $g(t)$  for  $t > t_1 = \tau$  has to be considered in more detail. For  $t \in I_1$  the follower is assumed to proceed with constant speed

$$v_{f,1} = v_{f,0} + \tau\alpha,$$

while the leader keeps on braking with rate  $\hat{B}$ . Hence,

$$g(t_1 + s) = g_1 + g'_1 s - \hat{B} \frac{s^2}{2}, \quad (21)$$

where

$$g'_1 = g'(t_1) = g'_0 - (\hat{B} + \alpha) \tau, \quad (22)$$

$$g_1 = g(t_1) = g_0 + (g'_0 + g'_1) \frac{\tau}{2}. \quad (23)$$

At the end of  $I_1$ , the gap's state has evolved to

$$g'_2 = g'(t_2) = g'_1 - \hat{B}\theta \quad (24)$$

$$g_2 = g(t_2) = g_1 + (g'_1 + g'_2) \frac{\theta}{2} \quad (25)$$

**Interval  $I_2$ .** Within  $I_2$  it is assumed that both vehicles decelerate with the rates  $B$  and  $\hat{B}$ , respectively. Thus,

$$g(t_2 + s) = g_2 + g'_2 s + \left(B - \hat{B}\right) \frac{s^2}{2}. \quad (26)$$

Since  $B > \hat{B}$ , the gap  $g(t)$  is concave for  $t > t_2$  until the follower stops. Consequently, a tangency may occur for an appropriate choice of  $\alpha$ . The requirement  $g'(t_{\parallel,2}) = 0$  yields

$$t_{\parallel,2} = t_2 + \frac{g'_2}{\hat{B} - B}. \quad (27)$$

Note that  $t_{\parallel,2} \geq t_2$  requires that

$$g'_2 \leq 0. \quad (28)$$

Using (27) in  $g(t_{\parallel,2}) = 0$  gives

$$g_2 = \frac{g'^2_2}{2(B - \hat{B})}.$$

Substituting (24)-(25) and applying the quadratic formula for  $g'_1$  gives

$$g'_{1,*} := \frac{1}{2} (B - \hat{B}) \tau + B\theta - \frac{1}{2} \sqrt{(B - \hat{B})^2 \tau^2 + 4(B - \hat{B})((\tau\theta + \theta^2)B + g'_0\tau + 2g_0)}. \quad (29)$$

Here the lower branch of solutions was selected since  $g'_1 \leq \hat{B}\theta$  is required from (28) and (24). Equation (29) yields a valid solution  $g'_{1,*} \leq \hat{B}\theta$  as long as

$$0 \leq \hat{B}(\theta\tau + \theta^2) + g'_0\tau + 2g_0 \quad (30)$$

From (27) we obtain

$$t_{\parallel,2} = t_2 + \frac{g'_{1,*} - \hat{B}\theta}{\hat{B} - B} \quad (31)$$

and if  $t_{\parallel,2} < t_{s,\ell}$  and Eq. (30) holds, the potential tangency in  $I_2$  acts limiting on  $\alpha$  implying an upper bound

$$\alpha_2 = \frac{g'_0 - g'_{1,*}}{\tau} - \hat{B}, \quad (32)$$

which is obtained by inserting  $g'_{1,*}$  into (22).

**Algorithmic choice of  $v_{\text{safe}}$ .** Summarizing the calculations of this section, we have developed the following procedure to calculate  $v_{\text{safe}}$  for the case  $B > \hat{B}$ :

1. Define  $v_{f,0} = v_f(t)$ ,  $v_{\ell,0} = v_\ell(t)$ , and  $g_0 = x_\ell(t) - x_f(t)$ .
2. Initialize a variable  $\alpha \leftarrow \infty$  [Eqn. (4)].
3. Determine  $t_{s,\ell}$  [Eqn. (14)]
4. Determine  $t_{\parallel,0}$  [Eqn. (18)]
  - (a) If  $t_{\parallel,0} \in (0, t_{s,\ell})$ , set  $\alpha \leftarrow \min \{\alpha, \alpha_{\parallel,0}\}$  [Eqn. (17)]
  - (b) Otherwise, set  $\alpha \leftarrow \min \{\alpha, (v_{\text{safe}} - v_{f,0})/\tau\}$  and proceed with step 8.
5. Check if a stop is required within  $I_0$ , i.e.,  $v_{f,0} + \alpha\tau \leq 0$ . If this is the case we can determine the vehicle's next state immediately:
  - (a) If  $t_{\parallel,0} \in (0, t_{s,\ell})$ , perform the state update according to Eqs. (19)–(20)
  - (b) Otherwise, perform the state update according to Eqs. (9)–(10)
6. Determine  $t_{\parallel,2}$  [Eqn. (31)]
  - (a) If  $t_{\parallel,2} \in (t_2, t_{s,\ell})$ , set  $\alpha \leftarrow \min \{\alpha, \alpha_{\parallel,2}\}$  [Eqn. (32)]
  - (b) Otherwise, set  $\alpha \leftarrow \min \{\alpha, (v_{\text{safe}} - v_{f,0})/\tau\}$
7. Determine the safe and maximal speed [Eqn. (4)] as

$$v_{\text{safe}} = v_{f,0} + \tau\alpha. \quad (33)$$

$$v_{\text{max}} = v_{f,0} + \tau a_{\text{max}}(v_{f,0}) \quad (34)$$

8. Use (33)–(34) to update the speed

$$v(t + \tau) = \min \{v_{\text{safe}}, v_{\text{max}}\}. \quad (35)$$

We summarize that there are five possible regimes governing a specific step  $(x_f(t), v_f(t)) \rightarrow (x_f(t + \tau), v_f(t + \tau))$  for the follower:

1. The original Gipps  $v_{\text{safe}}$  [Eqn. (7)] is selected:  $\alpha = (v_{\text{safe}} - v_f(t))/\tau$ .
2. The vehicle needs to perform a stop within  $I_0$  according to (19)–(20).
3. The maximal acceleration  $a_{\text{max}}(v_n)$  acts limiting:  $\alpha = a_{\text{max}}(v_n)$
4. The possible tangency in  $I_0$  acts limiting:  $\alpha = \alpha_{\parallel,0}$
5. The possible tangency in  $I_2$  acts limiting:  $\alpha = \alpha_{\parallel,2}$

The cases 1–3 are already present for the original Gipps model, while 4 and 5 are due to the additional class of constraints imposed by the possibility of tangent trajectories.

Figure 1(c) shows a scenario illustrating the dynamics of the extended Gipps model, where the follower employs the tangency avoidance scheme to prevent the collision shown in Fig. 1(a). The example shows a presumably desirable behavior as the follower smoothly approaches the minimal safe gap. However, it is important to point out that the parametrization of the model has to be taken out with some care. In particular, it is recommended to choose the (non-negative) parameter  $\theta$  of sufficient magnitude as very small values may lead to a 'bouncing' approach to a braking leader as illustrated in Fig. 3(a) and (b). In such a situation one or several subsequent tangencies can be observed due to an 'overshoot' leading to a larger gap than the minimal safe following gap at the end of the update step of length  $\tau$ . In Panel (a) a large overshoot can be observed due to a relatively large value of  $\tau = 2$  and vanishing  $\theta = 0$ . Intermediately, it even leads to a complete stopping. For smaller  $\tau$  the effect is still present though less obvious on the spatial level [see  $x(t)$  in the upper plot]. Nevertheless, an inspection of the evolution of the speed  $[v(t)]$  in the lower plot for  $\tau = 0.5$  shows abrupt changes of deceleration and acceleration in consecutive steps [see Fig. 3(b)]. The 'bouncing' effect can be effectively ameliorated by introducing  $\theta > 0$  [see Fig. 3(c)].



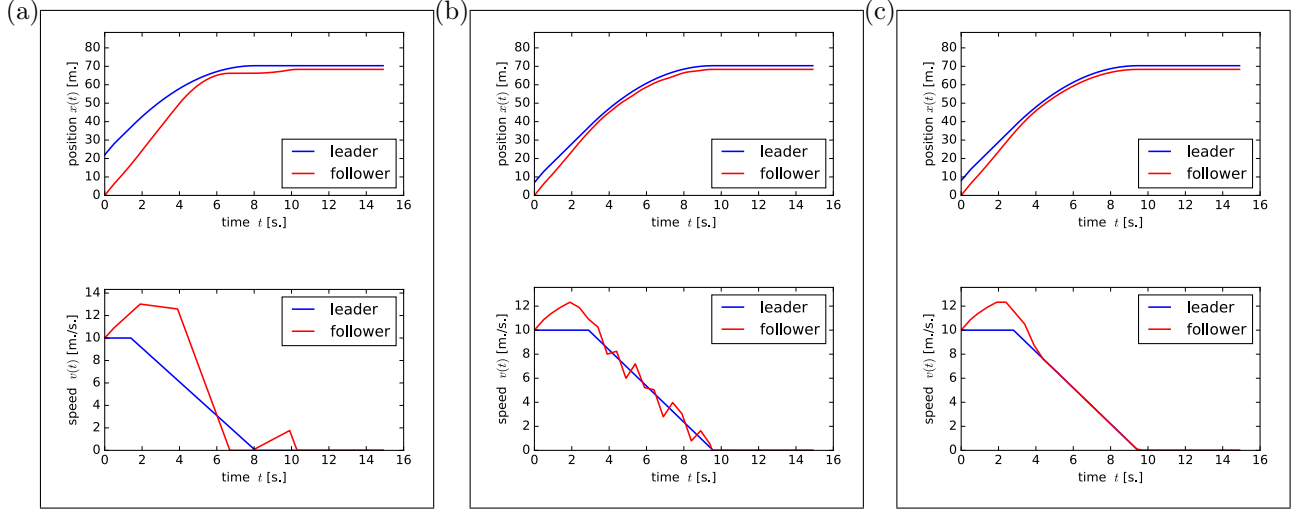


Figure 3: ‘Bouncing’ approach due to repeated tangential encounters of the follower’s and leader’s trajectories induced by too low values for  $\theta$  for the proposed extension of the Gipps model. Panel (a) shows a large tagental overshoot for  $\tau = 2$  and  $\theta = 0$ . Panel (b) shows that the phenomenon is present for smaller values of  $\tau$  as well, as can be seen from the evolution of the follower’s speed  $v_f(t)$  (red line in the lower plot). Panel (c) illustrates that the ‘bouncing’ is suppressed for non-vanishing  $\theta$  (here  $\theta = 0.1$ ,  $\tau = 0.5$ ). The experimental setup and the parameters were chosen as in Fig. 1 if not stated otherwise.

## 5 The Equilibrium Flow for the Case $B > \hat{B}$

In this section, we study the equilibrium flow in a system of several identical vehicle driver units, which obey the dynamics introduced in Sec. 4. Note that this implies that all drivers are disposed to brake with the same maximal comfortable rate  $B$ , while they estimate the leader’s maximal braking rate by  $\hat{B} < B$ . This means that all drivers are systematically underestimating their leader’s disposition for hard braking. Note that this does not automatically lead to an instability as shown in [13].

The equilibrium flow is a state of uniform speeds and inter-vehicle gaps, i.e.,

$$v_n(t) \equiv v_*, \text{ and } g_n(t) \equiv g_*,$$

where  $v_n$  is the speed of the  $n$ -th vehicle and  $g_n$  is its front gap. The front gap is defined as the remainder when subtracting a desired stopping distance  $g_{\text{stop}}$  from the bumper-to-bumper gap of the  $n$ -th vehicle and its leader, the  $(n + 1)$ -th vehicle. That is

$$g_n = x_{n-1} - l - g_{\text{stop}} - x_n,$$

where  $x_n$  is the  $n$ -th vehicle’s absolute position and  $l$  is the (uniform) vehicle length. A thorough analysis for the original Gipps model has been taken out by Wilson already [13]. Therefore we restrict our studies to situations, where the dynamics governing the equilibrium differ from (8). That is, we consider equilibrium solutions, where a possible tangency limits the safe next speed for the vehicle, see Sec 4. For the considerations below, studying the dynamics of the  $n$ -th vehicle as a follower of the  $(n - 1)$ -th vehicle at time  $t$ , such that the input parameters for determining the new speed  $v_n(t + \tau)$  of the follower are  $g_n(t)$ ,  $v_n(t)$ , and  $v_{n-1}(t)$ . These are to be identified with  $g_0$ ,  $v_{f,0}$ , and  $v_{\ell,0}$  from Sec. 4.

At first glance one may think there exist two different cases: one, where a tangency in  $I_0$  limits the acceleration and another, where a tangency in  $I_2$  poses the decisive constraint. However, in equilibrium flow we have  $g'_n(t) \equiv 0$ . Hence, no tangency can occur in  $I_0$  if not  $g_n(t) \equiv 0$ . We disregard this case in the following and restrict our analysis to equilibrium regimes  $(g_*, v_*)$  located within a neighborhood, where

$$v_n(t + \tau) = v_n(t) + \alpha_{\parallel,2}(g_n(t), v_n(t), v_{n-1}(t))\tau, \quad (36)$$

for all  $v_n(t)$  and  $v_{n-1}(t)$  sufficiently close to  $v_0$ , and all  $g_n(t)$  sufficiently close to  $g_*$ . This corresponds to the case that [cf. Eqs. (14) and (31)]

$$t_{\parallel,2} < t_{s,\ell} = v_*/\hat{B}. \quad (37)$$

We claim that in equilibrium this is equivalent to

$$\left(\frac{1}{\hat{B}} - \frac{1}{B}\right)^{-1} (\tau + \theta) < v_*. \quad (38)$$

To see that, first observe that  $g'(t) \equiv 0$  in the equilibrium. Therefore, from Eq. (32), we obtain

$$g'_{1,*} = -\hat{B}\tau. \quad (39)$$

Substituting this into (31) yields

$$t_{\parallel,2} = \frac{B(\tau + \theta)}{B - \hat{B}}. \quad (40)$$

Using (40) and (37) we obtain (38).

In the following we follow the notation used by Wilson [13] and consider a function  $F(\phi, \psi, \chi)$  defined such that

$$F(g_n(t), v_n(t), v_{n-1}(t)) := v_n(t + \tau), \quad (41)$$

where  $v_n(t + \tau)$  is computed by (36). Note that  $F$  still describes a *Gipps-like* model in the sense of Wilson [2001, p.3] since we have

$$\partial_\phi F > 0, \quad \partial_\psi F < 0, \quad \text{and} \quad \partial_\chi F > 0.$$

This is readily checked by substituting (32) into (36). In contrast to the original Gipps model, (41) has the form

$$F(\phi, \psi, \chi) = \chi + H(\phi, \chi - \psi), \quad (42)$$

with a function

$$H(\phi, \chi - \psi) := -\left(g'_{1,*}\right)_{|g_0=\phi, g'_0=\chi-\psi} - \tau\hat{B}, \quad (43)$$

depending merely on the gap  $g_0 = \phi$  and the speed difference  $g'_0 = \chi - \psi$  of the vehicles [cf. Eqn. (32) and (36)]. As a consequence the stationary gap  $g_*$ , which is approached when following a leader vehicle maintaining a constant speed  $v_0$ , is *independent of the speed*. Indeed,  $g_*$  is obtained as a solution of

$$v_* = F(g_*, v_*, v_*) = v_* + H(g_*, 0), \quad (44)$$

i.e.,  $H(g_*, 0) = 0$  implicitly defines  $g_*$  independently of the value of the stationary speed  $v_*$  [as long as (38) holds]. We obtain

$$g_* = \frac{(\tau + \theta)^2}{2} \left(\frac{1}{\hat{B}} - \frac{1}{B}\right)^{-1}. \quad (45)$$

The independence of the stationary speed of the stationary gap has important consequences. Firstly, an equilibrium solution with  $v_* < v_{\max}$  only exists in systems with a specific density of vehicles

$$\varrho_* = (g_* + l + g_{\text{stop}})^{-1}, \quad (46)$$

which allows to select uniform gaps of the exact magnitude  $g_*$ . In this case the homogeneous state can at most be neutrally stable since perturbations, which increase the speed of all vehicles homogeneously and simultaneously will persist. For lower densities  $\varrho < \varrho_*$  the stationary solution takes the form  $v_* = v_{\max}$  and  $g_n \equiv \varrho^{-1} - l - g_{\text{stop}} > g_*$  and is neutrally stable with respect to small perturbations in the gaps, i.e., also inhomogeneous gaps  $g_n$  are stationary with speed  $v_* = v_{\max}$  as long as  $g_n > g_*$ . For higher densities  $\varrho > \varrho_*$  and uniform gaps, i.e.  $g_n \equiv g < g_*$ , there exists no stationary speed  $v_*$  satisfying (44). Thus, for any equilibrium solution with gaps  $g < g_*$  the corresponding equilibrium speed  $v_*$  must violate (38), thus it is simply the equilibrium speed for the original Gipps model, given as [see Wilson, Eqn (3.14)]

$$v_* = \left(\frac{1}{\hat{B}} - \frac{1}{B}\right)^{-1} (\tau + \theta) \left(1 - \sqrt{1 - \frac{g}{g_*}}\right). \quad (47)$$

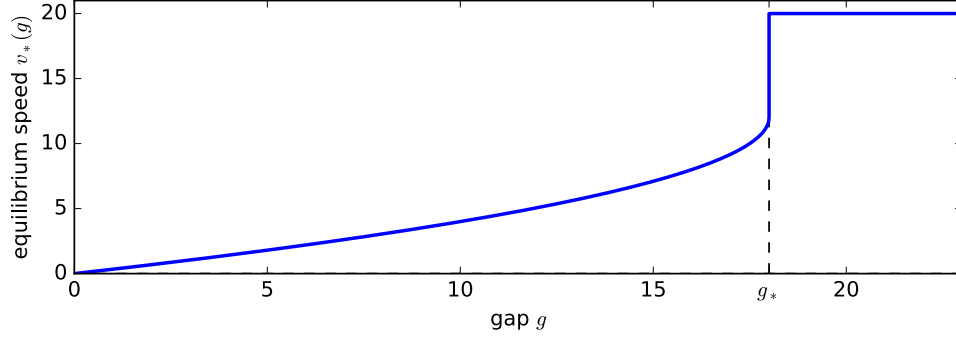


Figure 4: Dependence of the equilibrium speed  $v_*$  on the uniform gap  $g$  (speed-headway function). The dashed line indicates the critical value  $g = g_*$ , beyond which the mapping (36) is active and the vehicles go with maximum speed in the equilibrium flow. The model parameters for the illustration are the same as in Fig. 2, supplemented with  $v_{\max} = 20\text{m/s}$ .

Figure 4(a) shows the speed-headway function obtained from this reasoning. Note that it is the natural extension for the speed-headway function given by Wilson into the region defined by (38). It resolves the ambiguity of the original Gipps model in this region, which allowed for two different solutions. Interestingly, the function is discontinuous in  $g_*$ . Whether this is less “unphysical” than the multi-valued function encountered by Wilson is to be discussed. Punzo and Tripodi proposed speed-headway-density relations based on the original Gipps model, which resemble the shape but disregard the discontinuity [10]. [Optinally, we could elaborate on this a little]

## 6 Stability of the Equilibrium Flow

In the following we consider a circular track of length

$$L_N^* = \frac{N}{\varrho_*}, \quad (48)$$

with  $\varrho_*$  being the stationary density defined in (46), i.e., the track allows for equilibrium flows with stationary speed  $v_* < v_{\max}$  still fulfilling (38). This should be seen as an auxiliary construction to estimate the wave propagation within an array of vehicles traveling behind a slower leading vehicle with  $v_\ell < v_{\max}$ . In such a situation, the density  $\varrho_*$  will be approached locally within the array while traveling at lower speeds. Perturbations induced by irregularities of the leader’s trajectory will be magnified or damped according to the stability obtained for the equilibrium on the circular track.

To assess the systems stability, we study the system

$$\begin{pmatrix} v_n(t) \\ g_n(t) \end{pmatrix} \mapsto \begin{pmatrix} v_n(t+\tau) \\ g_n(t+\tau) \end{pmatrix} = \begin{pmatrix} F(g_n(t), v_n(t), v_{n-1}(t)) \\ G(g_n(t), v_n(t), g_{n-1}(t), v_{n-1}(t), v_{n-2}(t)) \end{pmatrix},$$

where all indices should be considered modulo  $N$  and

$$G(g_n, v_n, g_{n-1}, v_{n-1}, v_{n-2}) = g_n + \frac{\tau}{2} (v_{n-1} - v_n + F(g_{n-1}, v_{n-1}, v_{n-2}) - F(g_n, v_n, v_{n-1}))$$

describes the new front gap  $g_n(t+\tau)$  after the  $n$ -th vehicle has traveled for a time  $\tau$  with constant acceleration  $a_n = (v_n(t+\tau) - v_n(t))/\tau$ . The linearization of this map in a neighborhood of the equilibrium flow with

$v_n = v_* + \delta_n$ ,  $g_n = g_* + \eta_n$ , yields

$$\begin{aligned} F(g_n, v_n, v_{n-1}) &\approx v_* + DF_*(\eta_n, \delta_n, \delta_{n-1}) \\ &= v_* + \partial_\phi F_* \eta_n + \partial_\psi F_* \delta_n + \partial_\chi F_* \delta_{n-1}, \end{aligned} \quad (49)$$

$$\begin{aligned} G(g_n, v_n, g_{n-1}, v_{n-1}, v_{n-2}) &\approx g_* + DG_*(\eta_n, \delta_n, \eta_{n-1}, \delta_{n-1}, \delta_{n-2}) \\ &= g_* + \left(1 - \frac{\tau}{2} \partial_\phi F_*\right) \eta_n - \frac{\tau}{2} (1 + \partial_\psi F_*) \delta_n + \frac{\tau}{2} \partial_\phi F_* \eta_{n-1} \\ &\quad + \frac{\tau}{2} (1 + \partial_\psi F_* - \partial_\chi F_*) \delta_{n-1} + \frac{\tau}{2} \partial_\chi F_* \delta_{n-2}, \end{aligned} \quad (50)$$

with  $\partial_j F_* = \partial_j F(g_*, v_*, v_*)$ ,  $j = \phi, \psi, \chi$ . Next, we calculate the derivatives of  $F(\phi, \psi, \chi)$ . For notational convenience, we introduce a function

$$D(\phi, \chi - \psi) := \left(B - \hat{B}\right)^2 \tau^2 + 4 \left(B - \hat{B}\right) ((\tau\theta + \theta^2) B + (\chi - \psi) \tau + 2\phi).$$

This gives [cf. Eqn. (29)]

$$g'_{1,*} = \frac{1}{2} \left(B - \hat{B}\right) \tau + B\theta - \frac{1}{2} \sqrt{D(\phi, \chi - \psi)}. \quad (51)$$

Further note that from (39) it follows that in equilibrium we have

$$\sqrt{D(g_*, 0)} = B(\tau + 2\theta) + \hat{B}\tau. \quad (52)$$

Referring to Eqns. (42), (43), and (51), we calculate

$$\partial_j F(\phi, \psi, \chi) = \partial_j \chi + \frac{1}{4} \sqrt{D(\phi, \chi - \psi)}^{-1} \partial_j D(\phi, \chi - \psi), \quad j = \phi, \psi, \chi.$$

Thus, in equilibrium Eqn. (52) gives

$$\partial_j F_* = \partial_j \chi + \frac{\partial_j D}{4 \left(B(\tau + 2\theta) + \hat{B}\tau\right)},$$

where  $\partial_j D = 4 \left(B - \hat{B}\right) \partial_j ((\chi - \psi) \tau + 2\phi)$ . Defining

$$\xi := \frac{B - \hat{B}}{B(\tau + 2\theta) + \hat{B}\tau} > 0, \quad (53)$$

we find that

$$\partial_\phi F_* = 2\xi, \quad \partial_\psi F_* = -\tau\xi, \quad \text{and} \quad \partial_\chi F_* = 1 + \tau\xi. \quad (54)$$

Thus, (49) and (50) may be written as

$$DF_*(\eta_n, \delta_n, \delta_{n-1}) = 2\xi\eta_n - \tau\xi\delta_n + (1 + \tau\xi)\delta_{n-1} \quad (55)$$

$$DG_*(\eta_n, \delta_n, \eta_{n-1}, \delta_{n-1}, \delta_{n-2}) = (1 - \tau\xi)\eta_n - \frac{\tau}{2}(1 - \tau\xi)\delta_n + \tau\xi\eta_{n-1} - \tau^2\xi\delta_{n-1} + \frac{\tau}{2}(1 + \tau\xi)\delta_{n-2} \quad (56)$$

To determine the stability we determine characteristic multipliers  $\mu$  for the linearized system. That is solutions to

$$DF_*(\eta_n, \delta_n, \delta_{n-1}) = \mu\delta_n \quad (57)$$

$$DG_*(\eta_n, \delta_n, \eta_{n-1}, \delta_{n-1}, \delta_{n-2}) = \mu\eta_n. \quad (58)$$

The rotational symmetry of the systems suggests a rotating wave ansatz for the eigenmodes, i.e.,

$$\begin{pmatrix} \delta_n \\ \eta_n \end{pmatrix} = \omega_k^n \begin{pmatrix} \delta \\ \eta \end{pmatrix}, \quad (59)$$

with an  $N$ -th root of unity

$$\omega_k = \exp\left(\frac{2\pi k}{N} \cdot i\right),$$

where  $i = \sqrt{-1}$  and  $\eta, \delta \in \mathbb{C}$  are arbitrary complex numbers with  $\eta \cdot \delta \neq 0$ . Let us first consider the case that  $\eta = 0$ , which corresponds to unperturbed gaps. From (56) and (58) we obtain

$$-\frac{\tau}{2}(1 - \tau\xi) - \tau^2\xi\omega_k^{-1} + \frac{\tau}{2}(1 + \tau\xi)\omega_k^{-2} = 0. \quad (60)$$

Solving (60) for  $\omega_k^{-1}$  yields

$$\omega_k = \frac{\tau\xi + 1}{\tau\xi \pm 1},$$

which implies  $k = 0$ . Equations (55) and (57) give the corresponding multiplier

$$\mu_{0,1} = (1 + \tau\xi)\omega_k^{-1} - \tau\xi = 1.$$

As argued in Sec. 5 we obtain a neutrally stable mode corresponding a uniform variation of all vehicles' speeds.

For the calculation of the remaining multipliers we may assume that  $\eta \neq 0$ . Without loss of generality we set  $\eta = 1$ . Then, Eqs. (57)–(58) take the form

$$\mu\delta = 2\xi - \tau\xi\delta + (1 + \tau\xi)\delta\omega, \quad (61)$$

$$\mu = (1 - \tau\xi) - \frac{\tau}{2}(1 - \tau\xi)\delta + \tau\xi\omega - \tau^2\xi\delta\omega + \frac{\tau}{2}(1 + \tau\xi)\delta\omega^2, \quad (62)$$

where we let  $\omega = \omega_k^{-1}$ . Eqn. (61) yields

$$\delta = -\frac{2\xi}{(\omega - 1)\tau\xi - \mu + \omega}.$$

Using this in (62) gives:

$$\mu_{1,2} = h(\omega, \tau\xi) \pm \sqrt{h(\omega, \tau\xi)^2 - \omega}, \quad (63)$$

with  $h(\vartheta, \omega) = (\omega - 1)\vartheta + \frac{\omega+1}{2}$ . Note that  $\mu$  and thus the stability only depends on the product

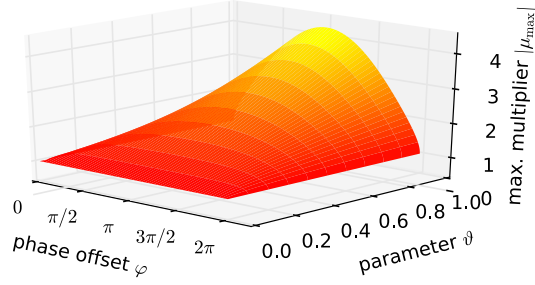
$$\vartheta = \tau\xi = \frac{B - \hat{B}}{B(1 + 2\theta/\tau) + \hat{B}}. \quad (64)$$

Figure 5(a) shows the larger of the two moduli  $|\mu_1|$  and  $|\mu_2|$  given in dependence of  $\vartheta$  and the argument  $\varphi$  of  $\omega = e^{i\varphi}$ . The numerical results support the conjecture that the maximal multiplier is obtained for  $\varphi = \pi$  independently of the value of  $\vartheta$ . An analogous observation was presented by Wilson for the case  $B \leq \hat{B}$ . We remind that the corresponding instability is a short wavelength instability, see [13, 3]. Figure 5(b) shows both curves  $\varphi \mapsto |\mu_j(\exp(i\varphi))|$ ,  $j = 1, 2$ , for  $\vartheta = 1.0$ . Similarly, for all values  $\vartheta > 0$  we obtain a branch  $|\mu_1| > 1$ . Hence the equilibrium flow for  $B > \hat{B}$  is unstable for all choices of parameters as long as Eqn. (38) is fulfilled. Indeed, numerical simulations suggest that collisions are unavoidable, which is not too surprising since all drivers systematically underestimate their leader's disposition to brake hard. Figure 6 shows two scenarios. In Panel (a) the track length is set exactly to  $L = L_N^*$  [see (48)] leading to an earlier collision. In Panel (b) the track length was increased such that each inter-vehicle gap increased by 2m. Interestingly, the direction of the wave emerging from the perturbation and ultimately leading to a collision propagates downstream, here. This stands in contrast to the wave in (a), which travels downstream.

## 7 Simulation Experiments

In this section we present some simulation results on a circular track for a set of 50 non-identical vehicles. In particular, we are interested in the situation where  $B > \hat{B}$  may arise without an assumption of underestimating  $\hat{B}$ . To this end we assumed that the values  $B_i$ ,  $i = 1, \dots, 50$ , for the different vehicles are uniformly

(a)



(b)

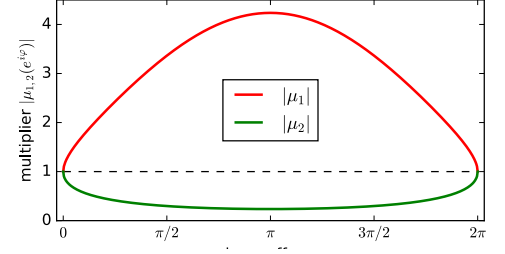
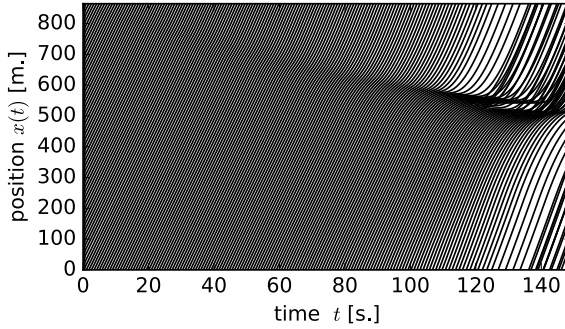


Figure 5: Plot (a): Maximal modulus  $|\mu_1(\omega)| > |\mu_2(\omega)|$  of the solutions of (61)–(62) in dependence of the parameter  $\vartheta = \tau\xi$  and the angle  $\varphi$  of  $\omega = e^{i\varphi}$ . The range  $\vartheta \in [0, 1]$  contains all reasonable parametrizations of the model, cf. (64). Plot (b) shows both multipliers  $\mu_{1,2}(e^{i\varphi})$  for  $\varphi \in [0, 2\pi]$ .

(a)



(b)

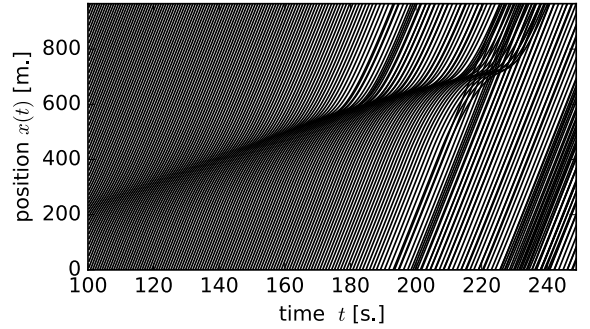


Figure 6: Collisions on a circular track with  $N = 50$  vehicles with initial speed  $v_0 = v_* + 1 \approx 21.8\text{m/s}$  for  $v_* = (\tau + \theta) \left( \frac{1}{\hat{B}} - \frac{1}{B} \right)$ , where  $\tau = 0.66$ ,  $\theta = 0.33$ ,  $B = 1.5$ , and  $\hat{B} = 1.4$ . Further, the maximal speed was set to  $v_{\max} = 30\text{m/s}$ . At  $t = 0$ , the vehicles are distributed uniformly on the track and one vehicle's initial speed is perturbed by setting it to  $\tilde{v}_0 = 0.9 v_0$ . For Plot (a) the track length is  $L = L_{50}^* \approx 865\text{m}$  [see (48)]. For Plot (b):  $L = L_{50}^* + 100\text{m}$ .

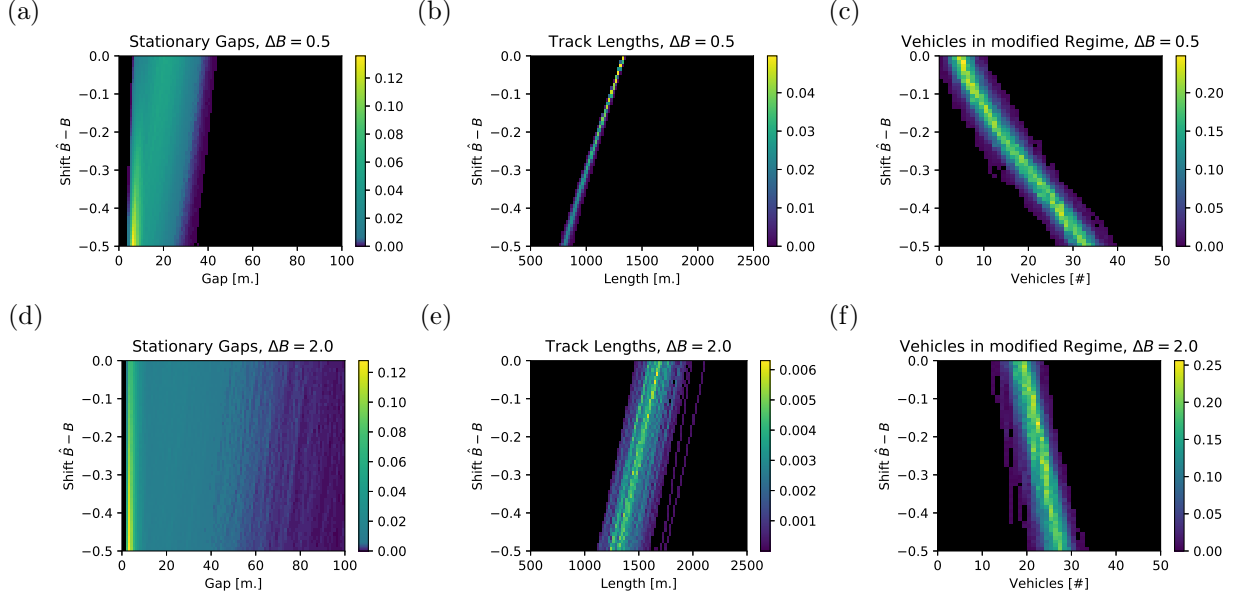


Figure 7: Distributions of different quantities related to the equilibrium flow in a heterogeneous ensemble of vehicles with stationary speed  $v_* = 20 \text{ m/s}$  for the model extension described in Section 4. The distributions obtained for different values of the bias  $\Delta \hat{B} = \hat{B}_i - B_i$  are shown as pixel rows and for two values of  $\Delta B$  ((a)–(c):  $\Delta B = 0.5 \text{ m/s}^2$ , (d)–(f):  $\Delta B = 2.0 \text{ m/s}^2$ , for both cases  $\bar{B} = 3.0 \text{ m/s}^2$ ). (a) and (d): Stationary gaps (including  $g_{\text{stop}} = 2.0 \text{ m}$ ); (b) and (e): Track lengths, cf. (65); (c) and (f): Number of vehicles for which the formula (45) is employed to determine the stationary gap.

distributed on an interval  $[\bar{B} - \Delta B, \bar{B} + \Delta B]$ . Further we varied the expected leader deceleration rates  $\hat{B}_i = B_i + \Delta \hat{B}$  by means of a constant, vehicle-independent bias  $\Delta \hat{B}$ . For a simulation with a particular realization of  $\mathbf{B} = (B_1, \dots, B_{50})$  we assumed the length of the circular track to be equal to

$$L(\mathbf{B}) = 50 \cdot (l + g_{\text{stop}}) + \sum_{i=1}^{50} g_{i,i+1}^*(v_*, B_i, \hat{B}_{i+1}), \quad (65)$$

where the stationary gap  $g_{i,i+1}^*$  between vehicle  $i$  and  $i+1$  is the smallest possible stationary spatial following headway, see Section 5. Figure 7 shows the distributions of  $L(\mathbf{B})$ ,  $g_{i,i+1}^*$ , and the number of vehicles where  $g_{i,i+1}^*$  is calculated according to the proposed extension, i.e., from (45), and differs from the stationary gap obtained for a conventional Gipps model. The distributions are normalized histograms generated from 500 realizations per value of  $\Delta \hat{B}$ .

For the stationary gaps [Fig. 7(a),(d)] the most pronounced feature is the accumulation of gaps at the lower bound of the distribution's support owing to the relatively small headways obtained for the case (45). By definition, this accumulation is correlated to the number of vehicles, for which (45) was employed, see (c) and (f). This is most clearly seen for the upper array of plots, where  $\Delta B = 0.5 \text{ m/s}^2$  is smaller as this number varies stronger with  $\Delta \hat{B}$  than for the case  $\Delta B = 2.0 \text{ m/s}^2$  shown in the lower array of plots. The small number of vehicles, for which the stationary gap is computed according to (45) for small  $\Delta \hat{B}$  [cf. (c)] follows from the fact that for small differences in  $B$  and  $\hat{B}$ , (45) is not employed, since for the hypothesized evolution of the headway  $g(t)$ , a tangency to  $g = 0$  is not possible until the leader has come to a full stop and the original formula used by Gipps still yields valid solutions. Although a stronger concentration of smaller headways can be observed for the case  $\Delta B = 2.0 \text{ m/s}^2$  [cf. (a) and (d)], the corresponding distributions of headways have longer tails leading to larger total sums, which determine the track lengths  $L(\mathbf{B})$ , cf. (b) and (e), as well as Eqn. (65).

Figure 8 shows the analogous results to those depicted in Fig. 7 for the case where the situation  $B > \hat{B}$  is resolved by assuming the leader's estimated braking rate to be not less than the followers, cf. (13). Note that this implies that for each pair of subsequent vehicles with  $B_{\text{follower}} > B_{\text{leader}} + \Delta \hat{B}$  this leads to an

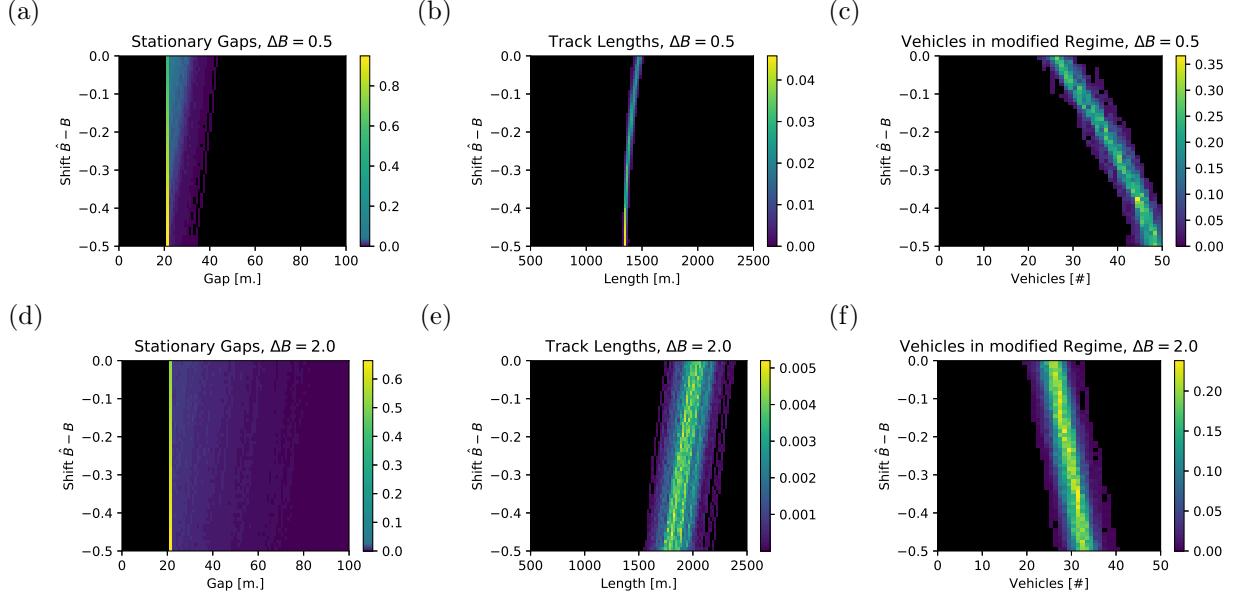


Figure 8: Distributions of different quantities related to the equilibrium flow in a heterogeneous ensemble of vehicles with stationary speed  $v_* = 20m/s$  obtained when resolving  $B > \hat{B}$  as in (13). Parameters:  $\bar{B} = 3.0m/s^2$ , (a)–(c):  $\Delta B = 0.5m/s^2$ , (d)–(f):  $\Delta B = 2.0m/s^2$ , cf. Fig. 7.

identical stationary headway of  $g_* = (\tau + \theta) \cdot v_*$ . This is the the reason for the vertical array of peaks in (a) and (d). It is clear that the resolution (13) will always lead to a larger stationary headway than the minimal safe headway as derived in Section 4, cf. Fig. 7(a),(d). This is also the reason for the larger total sum of headways observable in Fig. 8(b) and (e) when compared to Fig. 7(b) and (e).

Figure 9 shows a numerical stability experiment for the proposed extension of the Gipps model, where the magnitude of heterogeneity  $\Delta B$  and the error  $\Delta \hat{B}$  in the estimation of the leader's braking capability is varied. For each combination of the parameters we initialized the heterogeneous system in the stationary state for  $v_* = 20m/s$ . Then, we then perturbed this state by setting the initial velocity of a single vehicle to  $v_i(0) = v_* - \tilde{v}$ , with an initial perturbation  $\tilde{v} = 2m/s$ , and monitored the evolution of the maximal deviation  $\delta = |v_i(t) - v_*|$  of all vehicles' speeds from  $v_*$ . If the equilibrium flow was unstable, the perturbation would grow and the deviation could eventually reach its maximal possible value at  $v_* = 20m/s$ . This maximal deviation could be observed if stop-and-go waves emerged, where vehicles came to a total stop, or was imposed automatically if collisions were detected. For each parameter point, we executed several simulation runs of duration  $t_{\text{end}} = 1000s$ . (Fig. 9(a),(b)), resp.  $t_{\text{end}} = 500s$ . (Fig. 9(c)), with different realizations of  $B$ . Figure 9(a) and (b) show the destabilization regions in  $\Delta \hat{B}$  for fixed values  $\Delta B = 0.5$  and  $\Delta B = 2.0$ , respectively. To give an impression of the variability of the system's behavior across different realizations of  $B$ , we show several percentiles for the observed distributions of the deviation  $\delta$ , where we only considered times  $t > T/2$  for the calculation of  $\delta$ . In general, a value  $\delta > \tilde{v}$  indicates an instability of the equilibrium flow while  $\delta < \tilde{v}$  indicates stability. Notably, the case  $\Delta B = 2.0$  of larger heterogeneity exhibits a larger region of mixed stability as the case  $\Delta B = 0.5$  and the stabilization takes place earlier when varying  $\Delta \hat{B}$  from negative values towards the error-free case  $\Delta \hat{B} = 0$ .

Figure 9(c) shows a heatmap, whose color indicates the mean of the observed deviations  $\delta$  for a parameter region  $\Delta B \in [0.0, 2.0]$  and  $\Delta \hat{B} \in [-0.5, 0.0]$ . Each pixel represents a parameter combination and 50 corresponding simulation runs, which were initialized as described above and run for a duration of  $t_{\text{end}} = 500s$ . Two red bars indicate the one-dimensional parameter slices corresponding to (a) and (b). The crosses at  $\Delta B = 0.0$  indicate the values of  $\Delta \hat{B}$  for the homogeneous system, at which (i) the equilibrium flow of the classical Gipps ensemble destabilizes ( $\Delta \hat{B} \approx -0.142$ , cf. [13, Eqn. (5.13)]), and (ii),  $\Delta \hat{B} \approx -0.388$ , beyond which the equilibrium regime is governed by the tangential calculus, cf. condition (38). In accordance with the analytic results presented in Section 6 the equilibrium is unstable for  $\Delta \hat{B} < 0.388$  and  $\Delta B = 0.0$ . It may be observed that for all values of  $\Delta B$ , increasing the magnitude of the shift  $\Delta \hat{B}$  acts destabilizing. Though



this effect is clearly ameliorated for larger variations  $\Delta B$  of the maximal desired braking rates, indicating a stabilizing effect attributable to the ensemble heterogeneity.

## 8 Discussion

In the present work we introduced a novel, though canonic, approach to resolve collisions occurring in the Gipps car-following model, which was originally devised by the principle of choosing the maximal safe acceleration for the next simulation speed. Although mostly omitted, we assume that it is well known, that the safety principle fails in heterogeneous ensembles of vehicles, where the desired braking rates  $B_i$  of the different vehicles differ to a sufficient degree. We pinpointed the underlying reason for the collisions occurring in that situation and proposed a solution, which follows the original idea of travelling at a maximal safe speed. We kept the original form of Gipps' considerations for choosing the safe speed by assuming a three-partite continuation of a vehicle's trajectory into phases of constant acceleration, constant speed, and constant deceleration [cf. Section 3], and we showed that for some cases the maximal safe speed is not determined by the speed obtained from the Gipps model, but by a calculation of a tangency of the follower's distance  $g(t)$  to the leader in the hypothesized trajectory continuation, i.e., an occurrence of  $g(t_{\parallel}) = g'(t_{\parallel}) = 0$  for some  $t_{\parallel} > t$ . We analyzed the stability of the equilibrium flow in a regime, where the tangential calculus acts limiting on the stationary speed and found that it is always unstable. This is due to the requirement of a large underestimation  $\Delta \hat{B} = \hat{B}_i - B_i$  of the braking rate by interacting vehicles to 'activate' the corresponding regime. For heterogeneous ensembles, where the tangential case becomes relevant even without a misestimation of the braking rates, we conducted numerical stability experiments. Interestingly, these indicate an positive relation for the robustness of the equilibrium flow and the measure of heterogeneity. That is, stability is enhanced by heterogeneity.

One caveat for the proposed extension of the Gipps model is the singularity in the speed-headway relation obtained from the new regime, see Fig. 4, whose discontinuity does not meet the expectable form for this relation. A possible approach to handle this flaw might be the introduction of a speed dependence in the desired braking rate  $B(v)$ . Considering this characteristic, one may be tempted to retreat to the simpler strategy of resolving the collisions in the Gipps model by choosing always the maximum of  $B_i$  and  $\hat{B}_{i+1}$  for the calculation of the safe following speed as, for instance, exercised by the traffic simulation SUMO [7]. However, given standard assumptions this will always lead to a stable flow as instabilities require  $\hat{B}_{i+1} < B_i$  [13], and phenomena usually assumed to be related to instabilities must then be imposed as additional model components, see for instance the 'dawdling' in the Krauss model [8, 9].

Keeping these remarks in mind is especially important when one is concerned with simulations of safety aspects of traffic, such as simulated safety surrogate measures, for instance [CITE Gettman]. In any case, other possible ways to provoke unsafe or imperfect behavior of the Gipps model are assuming negative values  $\theta < 0$  for the reaction time buffer  $\theta$ , or values  $\tau < dt$  for the assumed reaction time  $\tau$ , which both may be interpreted as a driver's misestimation of the own reactive capabilities. Further, errors may be imposed on the input or output [8, 9, 5] of the model to achieve safety relevant deviations or plainly an increased realism for the model.

## References

- [1] Aimsun traffic modelling software. <https://www.aimsun.com/aimsun/>. Last visited 2017/06/29.
- [2] Paramics microsimulation. <http://www.sias.com/2013/sp/sparamicshome.htm>. Last visited: 2017/06/29.
- [3] M. Bando, K. Hasebe, A. Nakayama, A. Shibata, and Y. Sugiyama. Dynamical model of traffic congestion and numerical simulation. *Phys. Rev. E*, 51(2):1035–1042, February 1995.
- [4] Biagio Ciuffo, Vincenzo Punzo, and Marcello Montanino. Thirty Years of Gipps' Car-Following Model: Applications, Developments, and New Features. *Transportation Research Record: Journal of the Transportation Research Board*, 2315:89–99, December 2012.

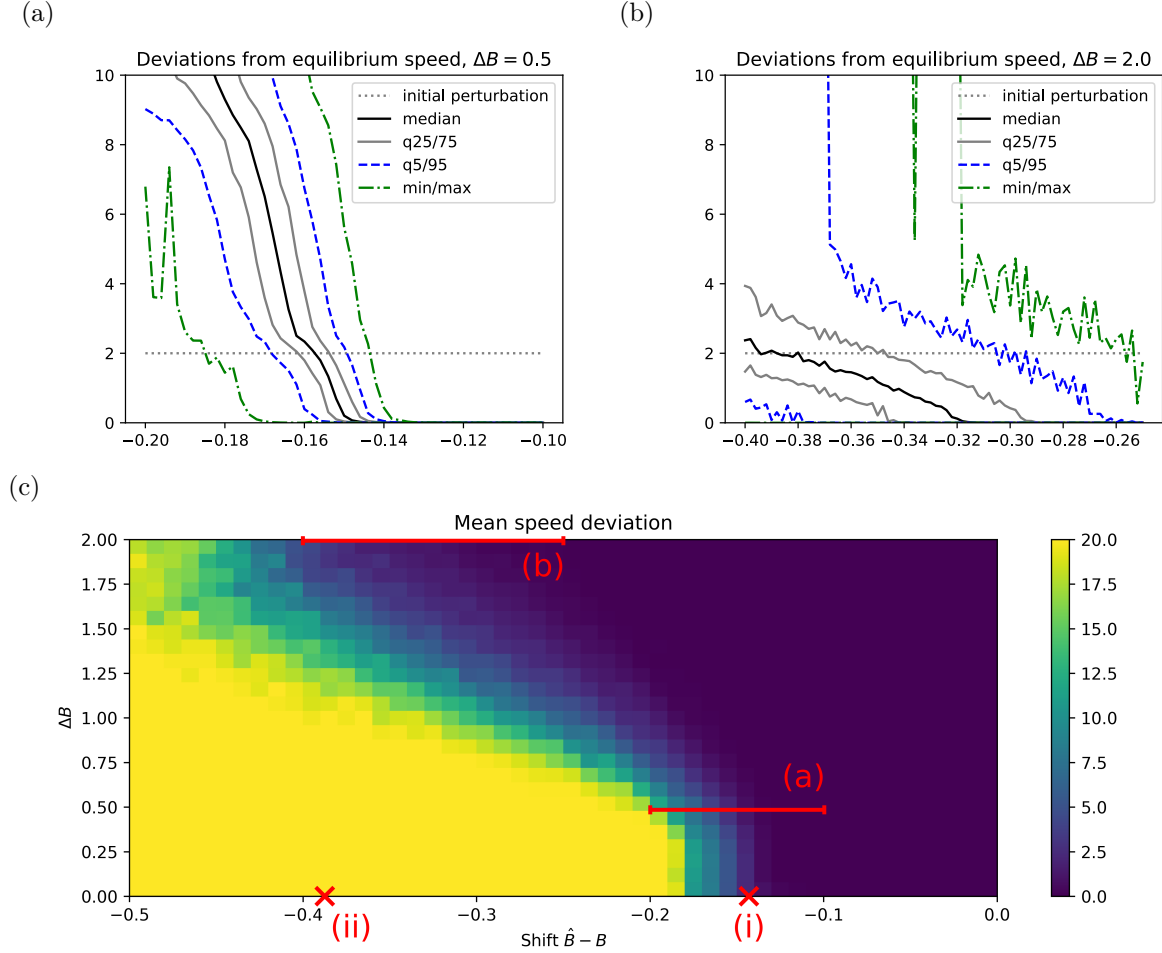


Figure 9: Observed stability of equilibrium flow for heterogeneous ensembles. (a) and (b): For two fixed values of the variability  $\Delta B$  several percentiles of the observed distribution of the speed deviation  $\delta$  from the equilibrium speed are plotted within a region, where the stability is lost for more than half of the samples  $B$ , i.e., the median of  $\delta$  exceeds the initial perturbation of  $2m/s$ . (c) Heatmap for the average deviation  $\delta$  from the stationary speed  $v_* = 20m/s$ . Higher (lighter) values at a coordinate indicate that, on average, the equilibrium is less stable, resp. more unstable, for the corresponding parameter combination than at coordinates exhibiting lower values. The intervals corresponding to (a) and (b) are indicated as well as to specific values of  $\Delta \hat{B}$  for the homogeneous system: (i) equilibrium stability switch, (ii) regime switch from classical Gipps to tangential calculus introduced in Section 4.

- [5] N. Eissfeldt and P. Wagner. Effects of anticipatory driving in a traffic flow model. *The European Physical Journal B - Condensed Matter and Complex Systems*, 33(1):121–129, May 2003.
- [6] P. G. Gipps. A behavioural car-following model for computer simulation. *Transportation Research Part B: Methodological*, 15(2):105 – 111, 1981.
- [7] Daniel Krajzewicz, Jakob Erdmann, Michael Behrisch, and Laura Bieker. Recent development and applications of SUMO - Simulation of Urban MObility. *International Journal On Advances in Systems and Measurements*, 5(3&4):128–138, December 2012.
- [8] S. Krauss, P. Wagner, and C. Gawron. Metastable states in a microscopic model of traffic flow. *Phys. Rev. E*, 55:5597–5602, May 1997.
- [9] Stefan Krauß. *Microscopic modeling of traffic flow: Investigation of collision free vehicle dynamics*. PhD thesis, 1998.
- [10] Vincenzo Punzo and Antonino Tripodi. Steady-State Solutions and Multiclass Calibration of Gipps Microscopic Traffic Flow Model. *Transportation Research Record: Journal of the Transportation Research Board*, 1999:104–114, 2007.
- [11] Martin Treiber and Venkatesan Kanagaraj. Comparing numerical integration schemes for time-continuous car-following models. *Physica A: Statistical Mechanics and its Applications*, 419:183 – 195, 2015.
- [12] Martin Treiber and Arne Kesting. *Traffic flow dynamics: data, models and simulation*. Springer Science & Business Media, 2012.
- [13] R. Eddie Wilson. An analysis of Gipps’s car-following model of highway traffic. *IMA Journal of Applied Mathematics*, 66(5):509, 2001.